P2.8 THE MECHANICS OF FALLING HAILSTONES AND HAILSWATHS

Kevin Vermeesch* and Ernest Agee
Purdue University, West Lafayette, IN

1. INTRODUCTION

This study has focused on the mechanics of falling hailstones and the ground swaths produced in supercell thunderstorm events. Although the complexities of cloud physics and the growth of hail embryos in supercell storms are critical to this research, a purely kinematic approach has been adopted. The reader is referred to Knight and Knight (2001) for an overview of hailstorms. This research had been divided into the following segments:

1) Mechanical equations for computing the terminal velocity of individual hailstones based on their
   a) size, shape, density, and mass
   b) height above the ground from which the hailstone is released
   c) density of air and drag coefficient for a range of Reynolds Number (Re) flows past falling hailstones

2) The supercell thunderstorm environmental wind has been mechanically imposed consisting of
   a) translational speed of the thunderstorm
   b) vertical profile of vertical velocity in the storm (through which the hail falls), and
   c) assumed axisymmetric mesocyclone flow field that produces torsion in the trajectory and left-side displacement of falling hailstones

3) Mechanical model calculations of hailswaths for a wide range of conditions (described above) including trajectories, torsion, and size sorting of hailstones, and

4) Observational evidence of hailswaths and their relationship to mechanical model calculations.

2. TERMINAL VELOCITY EQUATIONS

The terminal velocity, v_T, of a free-falling object in a gravitational field after t seconds can be calculated from Newton's Second Law of motion, and is given below as

$$v_T(t) = gt \tag{1}$$

for an object initially at rest and then released to fall through a vacuum where g is the acceleration of gravity. The presence of the atmosphere for a falling hailstone would cause one to rewrite Eq. (1) as v_T = *gt + drag force*. It can then be shown that

$$v_T(t) = \frac{1}{b}\sqrt{gmb}\,\tanh\left(\frac{t}{m}\sqrt{gmb}\right) \tag{2}$$

where b is given as

$$b = \frac{1}{2}C_D\rho_a A. \tag{3}$$

Here, C_D is the drag coefficient, ρ_a is the density of air, and A is the cross-sectional area of the hailstone. In Eq. (2) m is the mass of the hailstone, t is the fall time, and v_T represents a result of gravitational fall that is opposed by a drag force. Since falling hailstones achieve their maximum velocity on the order of seconds, Eq. (2) can be rewritten as

$$v_T = \left(\frac{2mg}{C_D\rho_a A}\right)^{\frac{1}{2}}. \tag{4}$$

Eq. (4) is the same as Eq. (6.1) in Knight and Knight (2001) and Eq. (9) in Matson and Huggins (1980) if one assumes spherical hailstones, and thus Eq. (4) becomes

$$v_T = \left(\frac{8g\rho_i r}{3C_D\rho_a}\right)^{\frac{1}{2}} \tag{5}$$

where ρ_i is the density of the hailstone and r is its radius.

* *Corresponding author address*: Kevin Vermeesch, Purdue University, Dept. of Earth and Atmospheric Sciences, 550 Stadium Mall Dr., West Lafayette, IN 47906; email: kvermees@purdue.edu

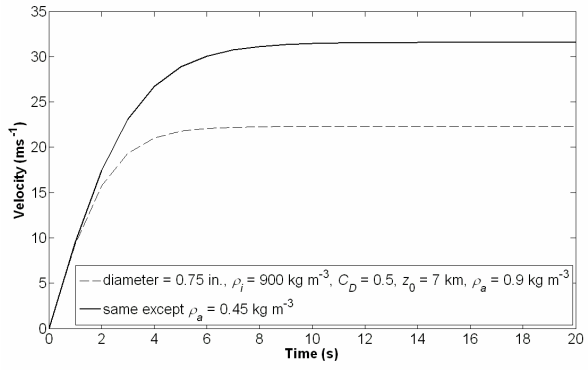

Figure 1. Plot of hailstone velocity versus time. The dashed represents the velocity of a hailstone with a diameter of 0.75 inches, a drag coefficient of 0.5, a hailstone density of 900 kg m^{-3}, a release height (z_0) of 7 km, and falling through air of constant density of 0.9 kg m^{-3}. The solid line represents the velocity of a hailstorm with same parameters except that the atmospheric density is 0.45 kg m^{-3}.

The solid line in Fig. 1 shows the achievement of terminal velocity for a ¾ inch spherical hailstone with ρ_i = 900 kg m^{-3}, ρ_a = 0.45 kg m^{-3}, C_D = 0.5, dropped from a height, z_0, of 7 km. The v_T of 31.5 ms^{-1} was achieved in 14.1 seconds with the total time to the ground of 224.1 seconds. The dashed line in Fig. 1 shows the similar result for a change in air density only to 0.90 kg m^{-3}, and thus a greater drag force. The v_T of 22.3 ms^{-1} was achieved in 9.5 seconds with a fall time to the ground of 315.3 seconds. These sample calculations show the effect of increased air density as well as the validity of allowing the hyperbolic tangent quantity in Eq. (2) to be approximated as 1, thus yielding Eq. (4) and Eq. (5) for spherical objects. The terminal fall velocities of hailstones for a variety of conditions for different air densities, hailstone diameters and densities, atmospheric release points, and different drag coefficients for laminar flows have been calculated and are consistent with Fig. 6.2 in Knight and Knight (2001).

Next, calculations of terminal fall velocities were made for hailstones released in a more-realistic atmosphere, with an exponential decrease in density with height,

$$\rho_a = \rho_0 \exp\left(-z/H_\rho\right) \qquad (6)$$

where H_ρ is the density scale height of 8.55 km, ρ_0 is the air density at ground level of 1.225 kg m^{-3}, and z is the height above ground level.

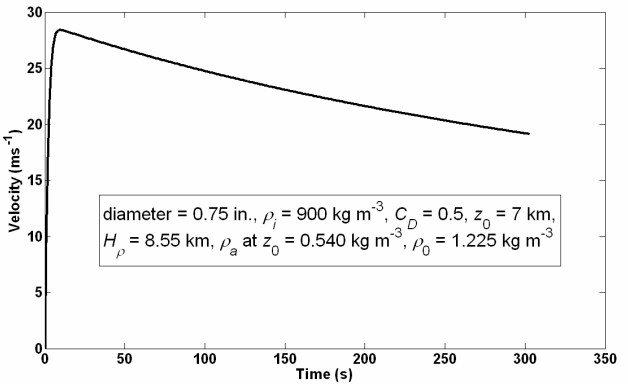

Figure 2. Plot of hailstone velocity as a function of time for a hailstone falling through an atmosphere in which ρ_a increases exponentially with decreasing height above the ground. The parameters of the hailstone and environment are given in the text box on the plot.

Fig. 2 shows the same result as the dashed line on Fig. 1, except the falling hailstone is encountering increasing drag and therefore decreasing v_T. The v_T at the ground decreases from 22.3 ms^{-1} to 19.2 ms^{-1}.

3. FALL VELOCITIES, TRAJECTORIES, AND HAILSWATHS FOR KINEMATIC CONDITIONS IN SUPERCELL STORMS

As indicated earlier, hailstones of various size, density, and shapes have been considered for an appropriate suite of kinematic conditions that are characteristic of supercell storms with large, damaging hailswaths. These kinematic features that affect the deposition of hail on the ground include translational speed, vertical velocity, and rotational speeds associated with an appropriately placed mesocyclone embedded in the supercell storm.

3.1 Spherical Hailstones and Sub-critical Re

The hailswaths presented here are for spherical hailstones ranging in diameter from one inch to two, three, and four inches. To describe a hailstone's trajectory (the fall path of the hailstone), it is first assumed that the hailstone is rotating in uniform circular motion at a distance R_C from the center of the mesocyclone. In uniform circular motion, the position vector as a function of time, $\vec{r}(t)$, (in a Cartesian coordinate system) of the hailstone is given by

$$\vec{r}(t) = (R_C \cos\theta(t))\hat{i} + (R_C \sin\theta(t))\hat{j} \qquad (7)$$

where $\theta(t)$ is the angle subtended at time t on the circumference of a circle with radius R_C and is given as

$$\theta(t) = \frac{v_\theta t}{R_C} \tag{8}$$

where v_θ is the tangential velocity of the mesocyclone. For simplicity in this preliminary stage of the study, the thunderstorm translational velocity vector is given as $\vec{V} = u\hat{i}$, so that the storm propagates only in an eastward direction. Substituting Eq. (8) into Eq. (7) and adding the translational position vector, $(ut)\hat{i}$, into Eq. (7) yields a three-dimensional position vector of a falling hailstone, given as

$$\vec{r}(t) = \left(R_C \cos\left(\frac{v_\theta t}{R_C}\right) + ut - R_C \right)\hat{i} + \left(R_C \sin\left(\frac{v_\theta t}{R_C}\right)\right)\hat{j} + \left(z_0 - (v_T t)\right)\hat{k}. \tag{9}$$

The R_C term is subtracted from the *x*-component because at time $t = 0$, the hailstone is positioned at $(0,0,z_0)$ and the center of the mesocyclone is located at $(-R_C,0)$. A schematic of the rotating and translating hailstone geometry is given in Fig. (3).

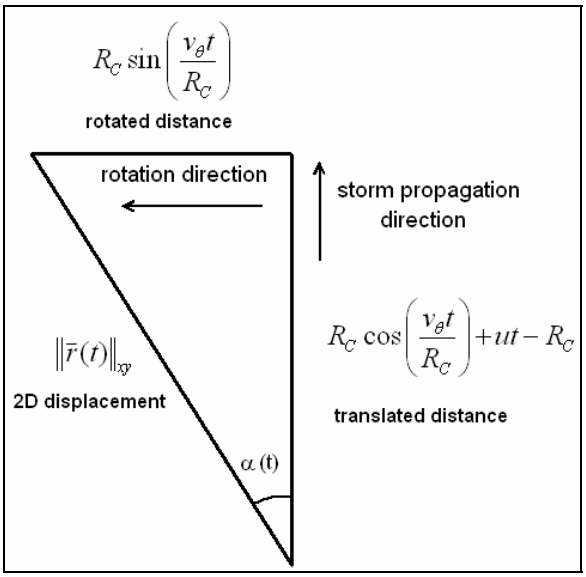

Figure 3. Two-dimensional geometry of the path of a rotating and translating hailstone. The storm is propagating to the east (towards the top of the figure) and the hailstone is rotating to the north (towards the left side of the figure). $\|\vec{r}(t)\|_{xy}$ is the resulting two-dimensional distance the hailstone has moved at time (*t*). $\alpha(t)$ is the angle the hailstone has rotated away from the mesocyclone center's path at time (*t*).

The angle the hailstone has rotated away from the center of the mesocyclone, $\alpha(t)$, is given by

$$\alpha(t) = \arctan\left(\frac{\|\vec{r}(t)\|_y}{\|\vec{r}(t)\|_x}\right) \tag{10}$$

where $\|\vec{r}(t)\|_x$ is the distance the hailstone has translated at time *t* and $\|\vec{r}(t)\|_y$ is the distance the hailstone has rotated (normal to the translational direction) at time *t*.

The hailstone is also assumed to be falling in a constant updraft, *w*, at this stage of the study. Since this upward air motion exerts another resistive force on the hailstone, Eq. (1) can be rewritten as $v_T = gt$ + *drag force* + *updraft force* and makes it necessary to modify Eq. (2) to accommodate the additional resistive force of the updraft. It can be shown that

$$v_T = \frac{\sqrt{(mg - w^2 b)b}}{b} \tag{11}$$

for $w \le \left(\frac{mg}{b}\right)^{\frac{1}{2}}$ after eliminating a hyperbolic tangent quantity (whose value approaches 1) as was done for Eq. (4). A falling hailstone trajectory produced by Eq. (9) is shown in Fig. 4 for a translating thunderstorm speed of 15 ms^{-1} and a constant *w* of 20 ms^{-1} for the entire hailstone descent. The release point of the hailstone is at 7 km above ground level (AGL) and the hailstones fall through a mesocyclone with a constant tangential velocity of 10 ms^{-1}.

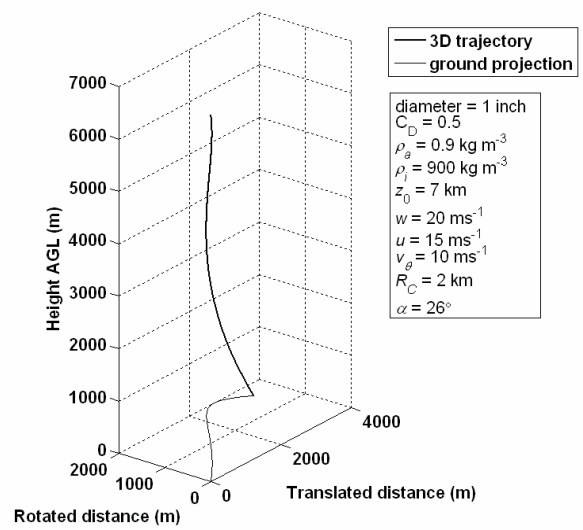

Figure 4. Falling hailstone trajectory and projected path on the ground produced by Eq. (9) with the parameters given in the text box on the right side of the figure and with a resulting angle of rotation of 26° to the left of the mesocyclone track (along the translated distance axis).

The combined effects of translation, rotation, and gravitational fall yield hailstone trajectories of various shapes or torsion. The projection on the ground of the center point of the mesocyclone is used as a reference point for determining the deposition of these hailstones for a translating, rotating thunderstorm event. This center point could also be assumed to be the location of the tornado if one should be present. As shown in Fig. (4), hailstones have limited turning angles which are to the left of the mesocyclone center (or tornado track) and are typically less than 90° with respect to the storm's path. Notice in Fig. 4 that the hailstone begins to rotate back towards the center of the mesocyclone. This phenomenon occurred in the model due to the constant tangential velocity with height and can occasionally occur in nature when an isolated hailstone may land behind or to the right of the tornado track. Since the hailstone has rotated a distance R_C away from the center of the mesocyclone and has not reached the ground, it begins to rotate toward the center along the back edge of the mesocyclone.

The size sorting of hailstones occurs in the hailswath when larger hailstones have faster terminal fall velocities and thus rotate a smaller distance away from the center of the mesocyclone before reaching the ground. This size sorting effect can be seen when hailstones of different sizes are dropped simultaneously as shown in Fig. 5.

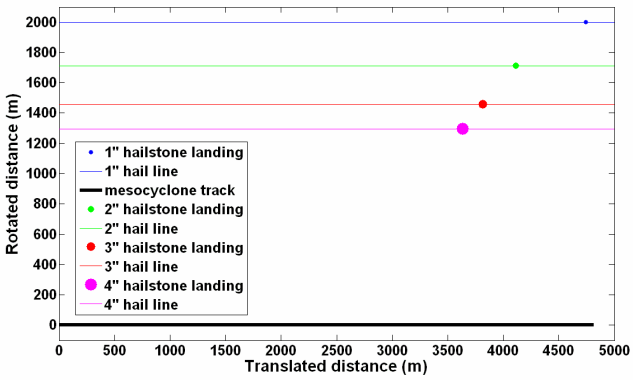

Figure 5. A model-generated size-sorted hailswath. Four hailstones ranging in diameter from 1 to 4 inches were simultaneously dropped using the hailstone and environmental parameters used in Fig. 4 except that an updraft speed of 15 ms^{-1} was used.

Some numerical results of Fig. 5 are given in Table 1. Notice that as the diameter of the hailstone increases, the angle of rotation and horizontal displacement decreases while the velocity with which the hailstone strikes the ground increases. All turning angles are reasonably close since the air density increased exponentially toward the ground. The reason for the smaller α of the 1 inch hailstone is because it has begun to rotate back towards the center of the mesocyclone. If it were not for this effect, the 1 inch hailstone would have a larger α than the 2 inch hailstone.

Table 1. Selected numerical results of the hailswath produced in Fig. 5. v_g is the velocity with which the hailstone reaches the ground and t_g is the fall time from the release point to the ground.

diameter (in)	1.0	2.0	3.0	4.0
v_g (ms^{-1})	16.21	27.41	35.27	41.57
t_g (s)	321	205	163	141
α (°)	36.05	38.97	38.70	38.35
$\left\|\vec{r}\right\|_{xy}$ (km)	3.40	2.72	2.33	2.09

3.2 Non-spherical Hailstones and Supercritical Re

As spherical hailstones grow to larger sizes, they develop knobs, lobes, and spikes which alter the flow of air around their surface. The increased surface roughness can make the hailstone transition from a laminar flow to a turbulent flow when the critical Re is exceeded. The turbulent flow reduces the air drag on the hailstone and thus lowers the drag coefficient, allowing the hailstone to achieve a faster terminal velocity. Up to this point in the study, a constant drag coefficient of 0.5 was used and was assumed to be representative of sub-critical Re values. To represent a hailstone falling in a

supercritical Re flow in this early stage of the investigation, the drag coefficient was reduced by half to 0.25, although further research is needed to determine a more-exact C_D-Re relationship between hailstones with varying surface roughness scales. A plot of the trajectory of a non-spherical hailstone with a drag coefficient of 0.25 is plotted with the trajectory of a spherical hailstone with a drag coefficient of 0.5 in Fig. 6. Although the non-spherical hailstone has spikes, the associated surface roughness length is assumed to be centered around the hailstone. This simplifying assumption still allows the spherical hailstone equation to be used, but for a reduced drag coefficient.

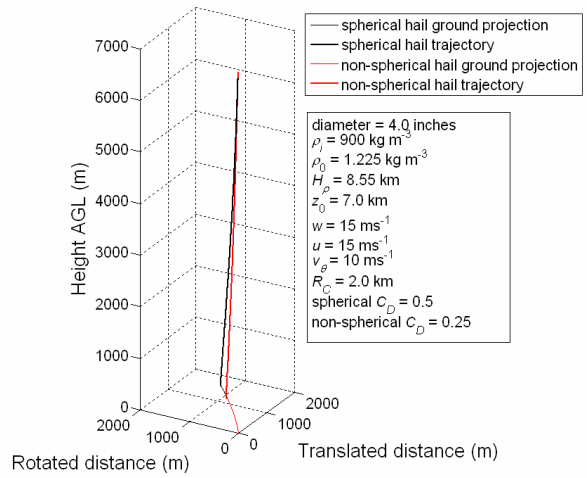

Figure 6. Trajectory of spherical and non-spherical hailstones. An exponential density increase with decreasing height AGL is used for ρ_a. The hailstone and environmental parameters are given in the box to the right of the plot.

In Fig. 6, both hailstones follow the same ground projection path but the spherical hailstone continues farther along the rotated path (that is, their ground projections overlap from the release point to the point of impact for the non-spherical hailstone although only one ground projection is visible in this portion of Fig. 6). In decreasing the drag coefficient by half, the velocity with which the hailstones strike the ground, v_g, increased from 41.6 ms^{-1} to 60.7 ms^{-1}, α decreased slightly from 38.3º to 37.4º, and $\left\|\vec{r}\right\|_{xy}$ decreased from 2.1 km to 1.6 km.

4. OBSERVED HAILSWATH AND FEATURES

As a preliminary and semi-quantitative verification of the hailstone position vector given in Eq. (9), documented hail and tornado reports from the 3 April 1974 Super Outbreak have been plotted using Google Earth software. These reports were obtained from questionnaires sent to the affected areas between May and August 1975 and from aerial tornado damage surveys. The exact locations of the reports are estimated from road intersections, geographic features, and the Google Earth satellite imagery. Other reasons to regard these reports as estimates is because the reports were obtained from the general public and the questionnaires were mailed to the respondents over a year after the event. Nevertheless, examination of Fig. 7 reveals evidence of a size-sorted hailswath. Fig. 7 is a portion of the Madison, IN F-4 tornado that began in southern Indiana in northern Clark County and tracked through southern areas of the town of North Madison, IN, ending in northeastern Jefferson County. While crossing the Madison area, the F-4 tornado inflicted heavy damage on the Hanover College campus, the Clifty Creek Power Plant (along the Ohio River), and the southern neighborhoods of North Madison.

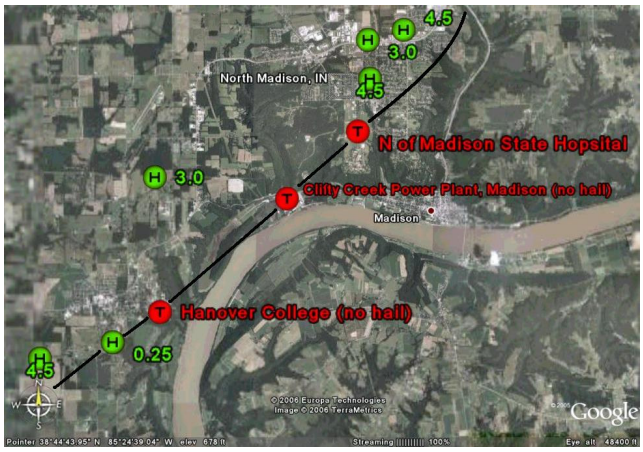

Figure 7. Reported locations of the Madison Tornado and associated hail on 3 April 1974 in southern Indiana plotted with Google Earth from damage surveys and questionnaire responses. The green dots represent hail reports and the diameter of the reported hail (in inches). The red dots are reported tornado locations. The heavy solid line is the estimated tornado path and the brown curve is the Ohio River separating Indiana (north and west of river) from Kentucky (south and east of river).

One can see that the larger hail reports are closer to the tornado track and the 0.25 inch hail report on the lower left corner of Fig. 7 was reported 15 minutes before the tornado struck that location. It is also important to note that it was reported that hail did not occur at Hanover College or the Clifty Creek Power

Plant, which were both directly struck by the tornado. Using the distance measuring tool in Google Earth, the 4.5 inch hail reports were located about 0.5 miles from the tornado path and the 3 inch hail reports were located about 0.9 to almost 1.5 miles to the left of the tornado path.

In comparing the hailswath in Fig. 7 to the model-generated hailswath in Fig. 5, it can be seen that there is a certain level of agreement between the two hailswaths, especially with the 3 inch hail report north of North Madison. This hail report was located about 0.9 miles (about 1.5 km) from the tornado track and the model-generated hailswath (using typical estimated values) placed the 3 inch hailstone almost 1.5 km from the center of the mesocyclone. A spatial gap between the hailstone reports and the tornado track is consistent with the model results shown in Fig. 5. To model this hailswath in more detail, estimates of the updraft velocity, mesocyclone radius, and rotational velocity, and translational velocity vector of the supercell thunderstorm that actually produced the Madison tornado would need to be estimated, as well as a high-density array of official hailstone size reports.

5. SUMMARY AND FUTURE WORK

Mechanical equations for hailstones that are falling in a rotating and translating updraft of a mesocyclone of a supercell thunderstorm have been developed to calculate the fall velocities of the hailstones and the hailswath they produce on the ground. Using the hail and thunderstorm properties given in Figs. 4 and 7, it was found that a size-sorted hailswath can be produced (Fig. 5) and is comparable to a documented hailswath (Fig. 7). It was also found that the hailstones rotate about 40º to the left of the center of the meoscyclone with velocities at the ground of about 20 to 40 ms^{-1} (with increasing speed as the diameter of the hailstone is increased) in a mechanically approximated thunderstorm kinematic environment. Taking into account the non-spherical properties of larger hailstones, because of a decreased drag coefficient if the critical Re is exceeded, the hailstone can increase the speed with which it strikes the ground from 60.7 ms^{-1} to 41.6 ms^{-1} for half the value of a spherical hailstone's drag coefficient.

Future work in this study will include a variable storm translational vector and vertical profiles of the updraft and rotational velocity. More research is also needed to parameterize the effect of supercritical Re flow depending on the oblateness of the hailstone. For further model verification, an officially reported hailswath will be used using hail data obtained from the Storm Prediciton Center's storm reports (or another high-resolution hail data set) combined with Doppler-derived rotational velocity values and hail core estimates. It is also desirable to use temperature sounding data to estimate the strength of the thunderstorm updraft.

6. ACKNOWLEDGEMENTS

This research is supported by gift funds from Mark and June Chen.

7. REFERENCES

Knight, C.A. and N.C. Knight, 2001: Hailstorms in *Severe Convective Storms*. *Meteor. Monograph*, **16**, No. 50., Amer. Meteor. Soc., 223-249.

Matson, R.J. and A.W. Huggins, 1980: The direct measurement of sizes, shapes and kinematics of falling hailstones. *J. Atmos. Sci.*, **37**, 1107-1125.